Title

Electrokinetic detection for X-ray spectra of weakly interacting liquids: n-decane and n-nonane

Journal

The Journal of Chemical Physics, 140(23)

ISSN

0021-9606

Authors

Lam, Royce K
Shih, Orion
Smith, Jacob W
et al.

Publication Date

2014-06-21

DOI

10.1063/1.4882901

Peer reviewed

AIP | The Journal of Chemical Physics

Electrokinetic detection for X-ray spectra of weakly interacting liquids: n-decane and n-nonane

Royce K. Lam, Orion Shih, Jacob W. Smith, Alex T. Sheardy, Anthony M. Rizzuto, David Prendergast, and Richard J. Saykally

Citation: The Journal of Chemical Physics **140**, 234202 (2014); doi: 10.1063/1.4882901
View online: http://dx.doi.org/10.1063/1.4882901
View Table of Contents: http://scitation.aip.org/content/aip/journal/jcp/140/23?ver=pdfcov
Published by the AIP Publishing

Electrokinetic detection for X-ray spectra of weakly interacting liquids: n-decane and n-nonane

Royce K. Lam,[1,2] Orion Shih,[1] Jacob W. Smith,[1,2] Alex T. Sheardy,[1,2]
Anthony M. Rizzuto,[1,2] David Prendergast,[3] and Richard J. Saykally[1,2,a)]
[1]*Department of Chemistry, University of California, Berkeley, California 94720, USA*
[2]*Chemical Sciences Division, Lawrence Berkeley National Laboratory, Berkeley, California 94720, USA*
[3]*Molecular Foundry, Lawrence Berkeley National Laboratory, Berkeley, California 94720, USA*

(Received 21 April 2014; accepted 30 May 2014; published online 16 June 2014)

The introduction of liquid microjets into soft X-ray absorption spectroscopy enabled the windowless study of liquids by this powerful atom-selective high vacuum methodology. However, weakly interacting liquids produce large vapor backgrounds that strongly perturb the liquid signal. Consequently, solvents (e.g., hydrocarbons, ethers, ketones, etc.) and solutions of central importance in chemistry and biology have been inaccessible by this technology. Here we describe a new detection method, upstream detection, which greatly reduces the vapor phase contribution to the X-ray absorption signal while retaining important advantages of liquid microjet sample introduction (e.g., minimal radiation damage). The effectiveness of the upstream detection method is demonstrated in this first study of room temperature liquid hydrocarbons: n-nonane and n-decane. Good agreement with first principles' calculations indicates that the eXcited electron and Core Hole theory adequately describes the subtle interactions in these liquids that perturb the electronic structure of the unoccupied states probed in core-level experiments. © *2014 AIP Publishing LLC*. [http://dx.doi.org/10.1063/1.4882901]

I. INTRODUCTION

The introduction of liquid microjets[1,2] into soft X-ray absorption spectroscopy (XAS) by Wilson *et al.* enabled applications to liquids.[3] Prior to this, soft XAS was restricted to ultra-high vacuum surface physics and gas phase studies. This methodology has since enabled the measurement of Resonant Inelastic X-ray Scattering (RIXS)[4,5] and Resonant Photoemission (RPE)[6,7] spectra of liquids, which provide complementary data to XAS. The use of liquid microjets also facilitates the study of liquids without attendant radiation damage, which can be a serious limitation. However, a gas phase background, resulting from the vapor jacket surrounding the liquid jet, is always present. This background is usually small relative to the primary liquid signal, comprising less than 10% of the total signal detected for aqueous samples, such that a straightforward subtraction of the gaseous signal is typically sufficient. However, weakly interacting liquids (e.g., hydrocarbons) have faster evaporation rates under high vacuum conditions that generate more extensive vapor jackets around the microjets, precluding meaningful characterization of the liquids. Total Electron Yield (TEY),[7–13] Total Ion Yield (TIY),[14,15] and Total Fluorescence Yield (TFY),[16–19] which comprise the most common detection schemes for XAS of liquid microjets, are all sensitive to the vapor background. New experimental modalities or new detection methods are therefore necessary to enable the study of weakly interacting liquids, which are important solvents in many chemical and biochemical contexts.[20–23]

This vapor background issue can potentially be addressed through the use of liquid flow cells, which have recently been used in XAS studies of a wide variety of systems.[24–26] These flow cells separate the liquid from the high vacuum environment through the use of silicon nitride windows. However, in the soft X-ray region, the windows attenuate the incoming X-ray beam, resulting in a significant reduction in signal, and they severely limit the study of nitrogen-containing compounds. Moreover, fluorescence detection must be used to detect the already-reduced signal and for low Z atoms, such as carbon, nitrogen, and oxygen, X-ray fluorescence is not the dominant de-excitation pathway.[27,28] Instead, the Auger process, which results in the ejection of electrons, is heavily favored as the core level de-excitation process. Therefore, it is usually preferable to detect via electron yield—especially when probing low Z atoms.

The use of liquid microjets in XAS provides important advantages over other existing methods for the study of liquids. This approach allows for windowless coupling to the X-ray synchrotron source, which ensures that the photon flux is not attenuated prior to interaction with the liquid. The microjet also provides a dynamic, rapidly renewed (microsecond residence times) sample which effectively eliminates sample damage. The signal generated by the impinging X-ray beam can then be detected via TEY, TIY, or TFY.

To reduce or eliminate the vapor background attending the use of liquid microjets, new detection techniques, motivated by optogalvanic[29,30] and electrokinetic[31–33] detection methods have been explored by our group. A schematic diagram of a typical microjet electrokinetics experiment is presented in Figure 1(a). A more detailed description of the microjet electrokinetics experiment has been published

a)Author to whom correspondence should be addressed. Electronic mail: saykally@berkeley.edu. Tel.: (510) 642-8269. FAX: (510) 642-8369.

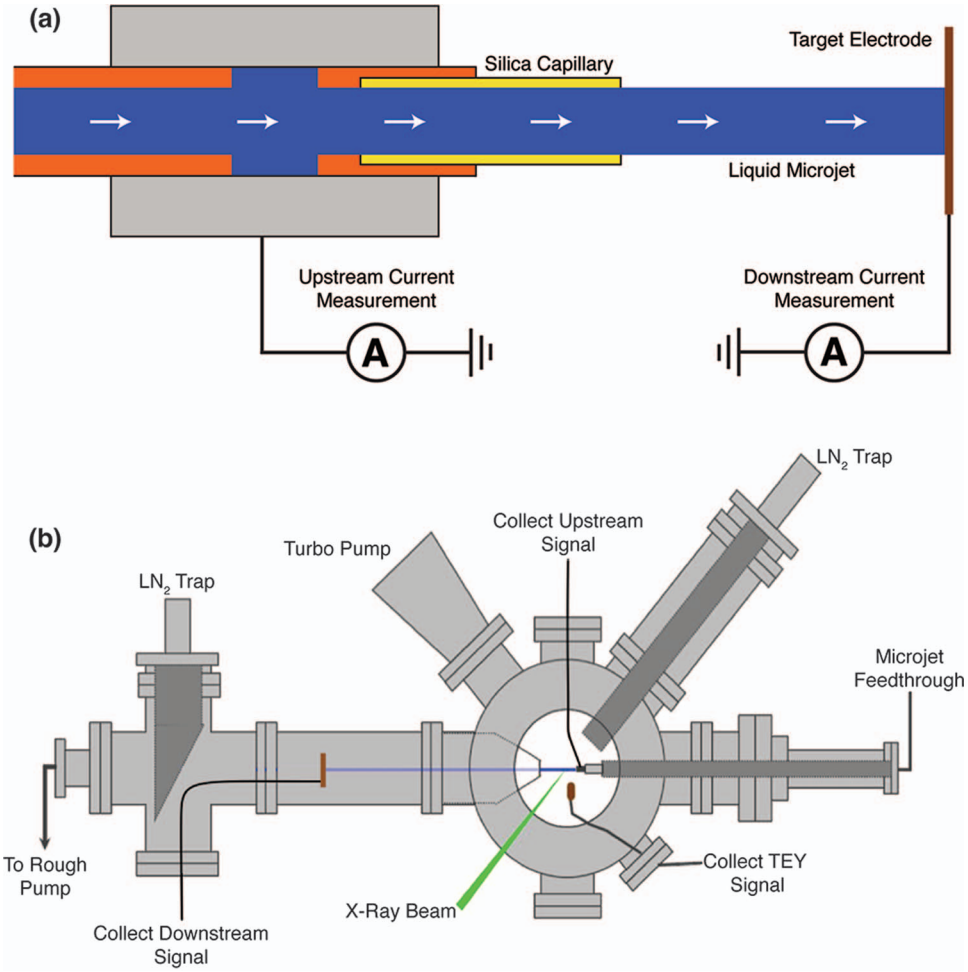

FIG. 1. Experimental schematics. (a) Schematic of microjet electrokinetics experiment. Streaming current can be simultaneously collected at the target electrode and upstream of the point of charge separation via back conduction. (b) *Downstream detection*: A heated metal plate was placed between the skimmer and liquid nitrogen trap. The downstream signal is collected concurrently with the TEY signal. *Upstream detection*: The standard silica capillary is replaced with a 50 μm stainless steel taper tip. The upstream signal is detected via the metal capillary concurrently with the TEY signal. Upstream and downstream detection schemes were not used concurrently.

previously.[31–33] Briefly, the current generated via charge separation at the microjet orifice can be detected both upstream, via back-conduction through the liquid, and downstream, on a target electrode. Analogously, we demonstrate in the present study that the X-ray absorption signal can be detected upstream of the impinging X-ray beam by measuring the magnitude of the charge present in the liquid jet following the removal of the ionized electrons by a positively biased electrode. Detecting downstream, while possible, proved to be impractical upon testing. The charge present in the liquid is proportional to the number of observed absorption events; hence, the method constitutes a novel type of "action spectroscopy" for core level spectroscopy.

II. METHODS

A. Samples

Water of 18.2 MΩ cm resistivity was obtained from a Millipore purification system. n-Nonane and n-decane with stated purity of at least 99% were obtained commercially from Alfa Aesar. Samples were used without further purification.

B. Experimental details

Oxygen and carbon K-edge TEY, downstream, and upstream spectra were collected at Beamline 8.0.1 at the Advanced Light Source (ALS) at Lawrence Berkeley National Laboratory. A detailed description of the X-ray experiment has been published previously.[9] Minor changes were made to accommodate the new downstream and upstream detection methods. Briefly, an intense ($>10^{11}$ photons/s), high resolution ($E/\Delta E = 7000$), and tunable soft X-ray beam is generated from an undulator at the ALS. The beam is then focused (100 × 35 μm spot size) onto a liquid jet. A syringe pump (Teledyne-ISCO 260D) drives the liquid through fused capillary tubing with a 30–50 μm inner diameter, creating a liquid jet with linear flow velocities in the range 1–200 m/s that is intersected with the X-ray beam in a high vacuum ($\sim 2 \times 10^{-4}$ Torr) chamber. The liquid beam then passes through a skimmer and freezes onto a cryogenic trap. A TEY signal is collected with a positively biased (2.1 kV) copper electrode located ~1 cm above the liquid sample as a function of photon energy. Vapor phase TEY spectra were collected by positioning the liquid microjet above or below the incident X-ray

beam. The recorded spectra were normalized to the current (I_0) collected from a gold mesh located further up the beamline to account for X-ray intensity variations.

To facilitate the new detection modalities, a straightforward modification was applied to our experimental endstation.[9] A schematic representation of the modified experimental design is shown in Figure 1(b). To enable the indirect detection of core-level absorption spectra downstream of the incident X-ray beam, a stainless steel target electrode, with an attached DC Peltier heater to prevent freezing, was placed between the skimmer aperture and the cryogenic trap. Current from the target was collected simultaneously with the TEY signal. To collect spectra upstream of the incident X-rays, the usual fused silica capillary is replaced with a 50 μm stainless steel taper-tip (New Objective). A wire is connected from the metal nozzle to a current amplifier (FEMTO DDPCA-300) to collect the upstream signal. The upstream spectrum is acquired simultaneously with the TEY spectrum. Simultaneous detection with TEY is essential to both the upstream and the downstream detection schemes. The removal of the ionized electrons by the positively biased electrode results in a positively charged liquid jet. The magnitude of the positive current can then be measured both upstream or downstream of the incident X-ray beam. The exact mechanism of conduction through the resistive liquid for the upstream detection is presently undetermined although induction is likely. Upstream and downstream signals were not collected concurrently.

C. Calculations

Gromacs 4.6.4[34–38] was used to perform classical NVT MD simulations of both gas phase and liquid n-decane. The gas phase system contained a single decane molecule in a cubic box of edge 30.000 Å and the liquid system contained 30 molecules of decane in a periodic cubic box of edge 21.280 Å. The simulations employed a modified OPLS-AA[39–41] forcefield developed by Siu *et al.*[42] Following an initial minimization, the liquid system was heated to 298 K and then equilibrated for 500 ps under constant pressure to a final density of 0.736 g/ml. An NVT simulation was then run for 2 ns. For the gas phase system, an NVT simulation was run immediately following heating to 298 K. The molecular configuration of each system was collected every 20 ps for use in the spectral simulation.

To calculate the X-ray absorption spectrum, atomic coordinates were taken from the final snapshot of the NVT simulation of liquid decane and from 10 uncorrelated snapshots of the single molecule NVT simulation for gas phase decane. The core level excitation linestrengths were calculated with the eXcited electron and Core Hole (XCH) density functional theory approach.[43] The electronic structure was calculated using the plane wave self consistent field (PWSCF) code from the Quantum-ESPRESSO package.[44] The exchange correlation energy was estimated with the Perdew-Burke-Ernzerhof (PBE) exchange correlation functional within the generalized gradient approximation.[45] A plane wave basis set with periodic boundary conditions and a kinetic energy cut-off of 25 Ry was used to model the localized and delocalized states. In the XCH approach, the lowest core-hole excited state is explicitly treated. The resulting self-consistent field was used to generate higher excited states non-self consistently. Transition amplitudes were then calculated within the single-particle and dipole approximations. The calculated transitions are broadened by Gaussian convolution of 0.1 eV full width half maximum. The energy axis was aligned relative to the experimentally collected vapor phase spectra of decane and a similarly calculated spectrum for a single decane molecule. Isosurfaces were calculated with Quantum-ESPRESSO and rendered in VESTA.[46]

III. RESULTS AND DISCUSSION

Detecting the signal downstream of the incident X-rays, while possible, proved to be problematic. The addition of the DC heater to mitigate freezing in the high vacuum environment resulted in the crystallization of solutes onto the target. This led to a rapid degradation in the target electrode conductivity and the ability to detect changes in the charge carried by the liquid jet. Additionally, the natural breakup of the liquid jet due to Rayleigh instabilities[47,48] and evaporation in the vacuum chamber often prevented the charged liquid from reaching the target electrode. Due to these issues, downstream detection of the X-ray signal as a method of reducing the vapor background was deemed impractical.

Detecting the X-ray absorption signal upstream of the impinging X-rays proved to be a more viable approach. By using a metal capillary as the detection electrode, the issues that arose from the downstream detection, freezing on the target electrode, crystallization of dissolved solutes, and vaporization of the liquid jet prior to detection, were entirely eliminated. The upstream detection scheme was first tested on the well-studied liquid water system[3,49] and then on liquid nonane and liquid decane. These weakly interacting, long-chain liquid hydrocarbons are not typically considered to be highly volatile liquids, but since they exhibit high evaporation rates under high vacuum conditions, they essentially behave as such. As a result, in previous attempts to measure X-ray absorption spectra of liquid long-chain alkanes using microjets, only vapor phase spectra were collected.

Figure 2 compares the oxygen K-edge core level spectra of liquid water collected via both TEY and upstream

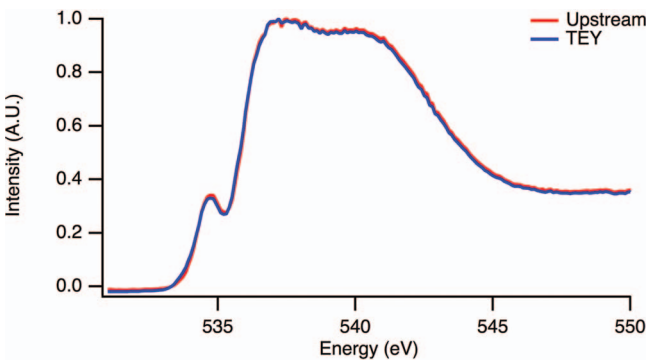

FIG. 2. Oxygen K-edge absorption spectra for 25 °C liquid water measured simultaneously with TEY and upstream detection. Spectra have been normalized to the peak maximum for direct comparison.

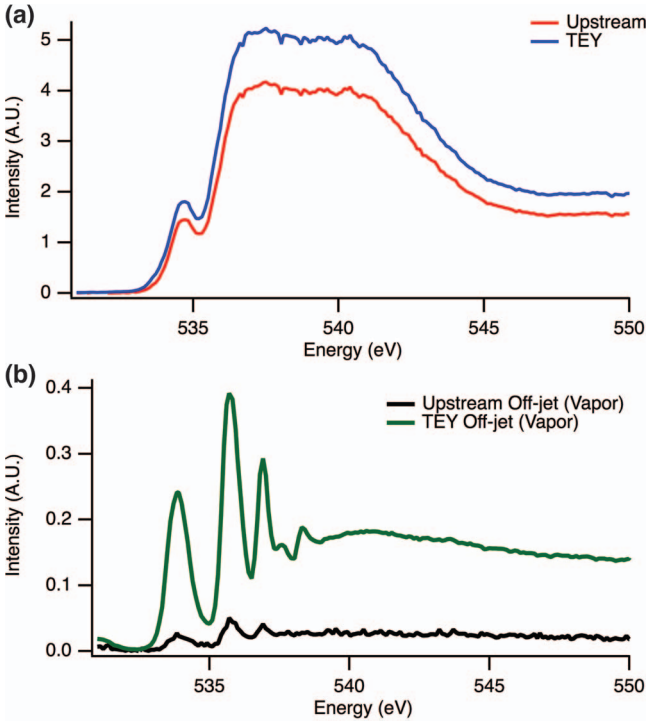

FIG. 3. Unnormalized oxygen K-edge absorption spectra for 25 °C water measured simultaneously with TEY and upstream detection. (a) On-jet (liquid) spectra; (b) off-jet (vapor) spectra. The off-jet signal originates from the liquid microjet vapor jacket.

detection. The spectra are normalized to the intensity of the strongest peak to facilitate direct comparison. As expected, due to the thin vapor jacket surrounding the water jet, the on-jet spectrum of liquid water is identical for the two detection methods. However, comparison of the unnormalized liquid (on-jet) and vapor (off-jet) spectra, shown in Figure 3, reveals a significant difference in the two detection schemes. While the upstream detection exhibits only a slightly reduced sensitivity to the signal originating in the liquid, it exhibits a significantly reduced sensitivity to the signal from the microjet vapor jacket. Overall, there is a five-fold increase in the liquid/vapor signal contrast in the upstream spectrum and similar signal-to-noise ratios when compared to TEY detection. The ∼20% decrease in the signal intensity in the upstream spectrum is likely a result of the inefficiencies in the mechanism of charge transfer back through the liquid.

In prior attempts to measure X-ray absorption spectra of liquid hydrocarbons using liquid microjets with TEY, shown in Figure 4(a), the area normalized on-jet and off-jet spectra appeared essentially identical, whereas for strongly interacting liquids, like water and methanol, the liquid-phase spectrum is distinctly different from that of the gas and solid phases.[3,50–52] The anticipated broadening and spectral changes normally associated with the transition from the gas phase to the liquid phase spectrum were not observed in the hydrocarbon TEY spectra shown above. There are two possible explanations for this invariance between the liquid and vapor spectra observed previously. The first is that there genuinely is no difference between the gas phase and condensed phase spectra. Liquid hydrocarbons interact primarily through dispersion and weak electrostatic forces.[42,53–55] It is possible that these interactions are simply not strong enough to exert an observable influence on the energy levels of the unoccupied orbital states of the molecule that are probed in the X-ray experiment. However, the increased density in the liquid phase should result in inhomogeneous, collisional broadening that should be clearly evident in the liquid spectrum at the high resolution of the present X-ray experiments. A more likely explanation for the similarities between the previously measured absorption spectra is simply that the signal arising from the vapor surrounding the microjet overwhelms the on-jet TEY spectrum. Liquid nonane exhibits an evaporation rate in a high vacuum environment that is significantly greater than those of the typical systems studied using liquid microjets (primarily aqueous solutions and alcohols).[2,50] The faster evaporation rate thus leads to a higher local vapor pressure surrounding the microjet and thus a larger vapor signal component in the on-jet spectrum.

Because the upstream detection method is much less sensitive to the signal originating from the vapor jacket, it can more effectively sample the genuine liquid phase spectra of samples with high local vapor pressures. Newly detected carbon K-edge X-ray absorption spectra of liquid nonane and decane are shown in Figures 4(b) and 4(c). The spectra shown have been area normalized to allow for the comparison of peak intensity changes and shifts between the liquid and vapor phase. In these newly obtained spectra, clear differences are apparent between the on-jet (upstream and TEY) and the off-jet (TEY) vapor signal. In the on-jet (liquid) spectra, the feature centered near 292 eV is significantly broadened (FWHM: 2.13 eV for vapor; 4.25 eV for TEY; 5.45 eV upstream for decane) and slightly blueshifted (TEY: 0.42 eV; upstream: 0.80 eV for decane) relative to the off-jet spectra. A significant reduction (∼40%) in intensity of the feature near 292 eV is observed in the liquid phase spectra. More importantly, the upstream spectra are more blueshifted and broadened, and exhibit a greater reduction in peak intensity than the do TEY on-jet spectra, indicating that the upstream signal exhibits a significantly reduced sensitivity to the vapor, and therefore a far more genuine liquid-phase signal.

To interpret the experimental X-ray absorption spectra, calculations were performed using the XCH density functional theory approach[43] described above for both gas phase and liquid phase decane. As the measured spectra for nonane and decane exhibit nearly identical spectral features, shown in Figure 4(d), the analogous XCH calculations were not performed for nonane. Due to the inherent similarities between the liquid and vapor spectra, the first two peaks, centered at 287.2 eV and 287.7 eV were assigned by comparing to the calculated spectrum for a single decane molecule, as shown in Figure 4(e). The two peaks correspond to the C (1s) → σ^* (C–H) and C (1s) → σ^* (C–C) transitions, respectively. Unlike the broad feature centered near 292 eV, these two peaks are not significantly blueshifted in the liquid. This indicates that the LUMO and LUMO+1 states are not appreciably perturbed by intermolecular interactions in the liquid phase. In contrast, the broad feature centered at 292 eV arises from many highly mixed and delocalized states. The calculated spectrum of liquid decane exhibits the same broadening, shift,

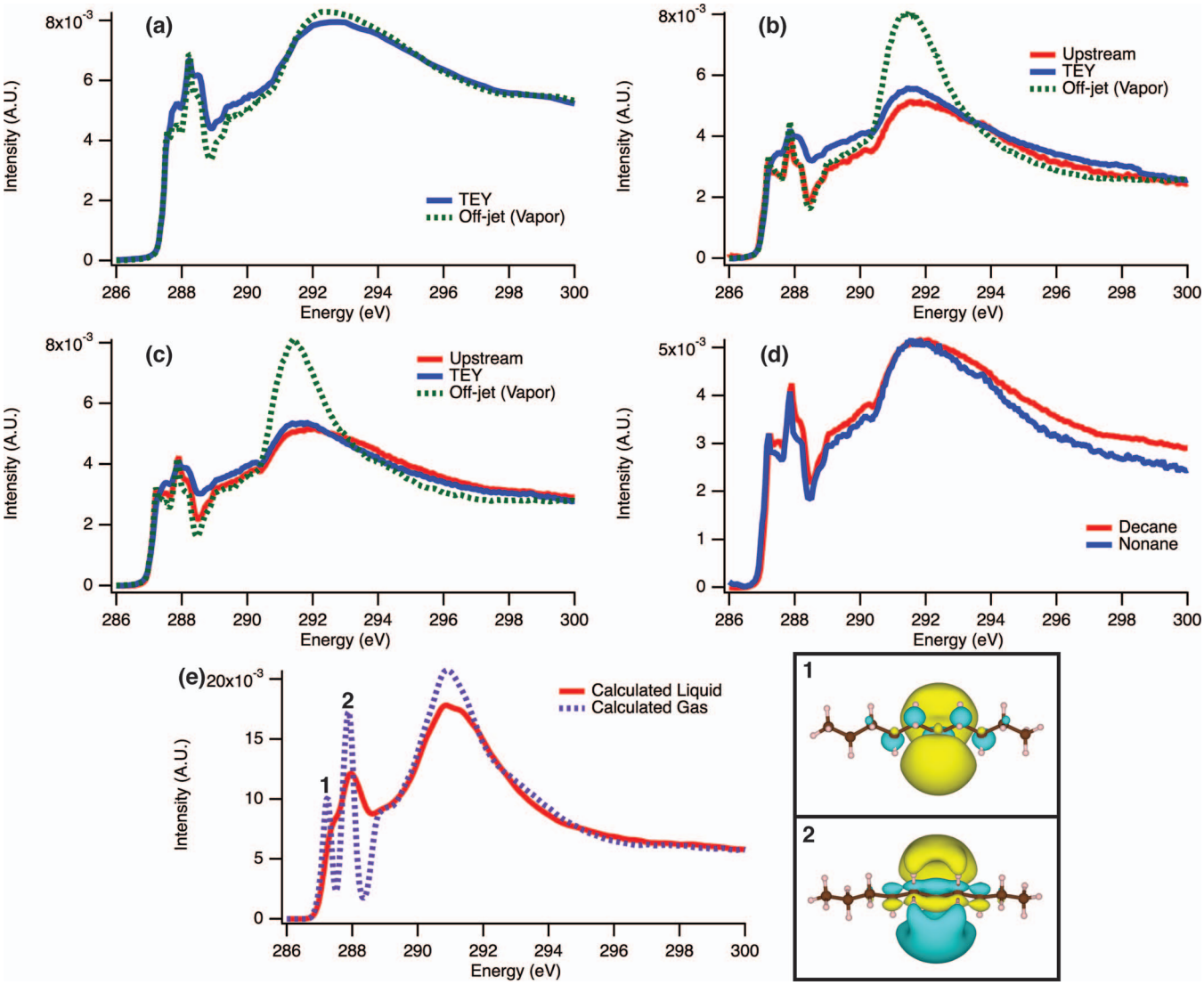

FIG. 4. Carbon K-edge X-ray absorption spectra for n-nonane and n-decane. All experimental spectra have been area normalized. (a) Previously measured carbon K-edge absorption (TEY) spectra of n-nonane. Off-jet signal, shown in green, is the vapor signal originating from the microjet vapor jacket. (b) Carbon K-edge absorption spectra of n-nonane measured simultaneously with TEY and upstream detection. Off-jet signal, shown in green, is the vapor signal originating from the microjet vapor jacket. FWHM: off-jet: 2.70 eV; TEY: 3.24 eV; upstream: 4.26 eV. Blueshift relative to off-jet: TEY: 0.11 eV; upstream: 0.30 eV. (c) Carbon K-edge absorption spectra of n-decane measured simultaneously with TEY and upstream detection. Off-jet signal, shown in green, is the vapor signal originating from the microjet vapor jacket. FWHM: Off-jet: 2.13 eV; TEY: 4.25 eV; upstream: 5.45 eV. Blueshift relative to off-jet: TEY: 0.42 eV; upstream: 0.80 eV. (d) Comparison of carbon K-edge liquid phase spectra of nonane and decane measured with upstream detection. (e) Comparison of the calculated carbon K-edge spectra for gas phase decane and liquid decane. Peak 1 ($1s \rightarrow \sigma^*$ (C–H), 287.2 eV) and peak 2 ($1s \rightarrow \sigma^*$ (C–C), 287.8 eV).

and reduction in intensity as the experimental spectrum. The broadening observed in the liquid phase spectra of nonane and decane is primarily a result of inhomogeneous broadening, since the liquid linewidths considerably exceed the gas phase linewidths, which are dominated by the core hole lifetimes.

IV. CONCLUSIONS

Using the new upstream detection approach, unperturbed spectra of two weakly interacting liquids, n-nonane and n-decane, were obtained and exhibit very good agreement with spectra calculated from first principles' theory. With this windowless approach, we are able to retain all of the advantages gained from the use of liquid microjets while effectively suppressing the gas phase background. With less volatile liquids, such as water, an essentially complete elimination of the gas phase background is observed. This opens the way for general study of this new class of liquids and solutions.

ACKNOWLEDGMENTS

This work was supported by the Director, Office of Basic Energy Sciences, Office of Science, U.S. Department of Energy (DOE) under Contract No. DE-AC02-05CH11231, through LBNL Chemical Sciences Division. Computational resources were provided by the National Energy Research Scientific Computing Center (NERSC), a DOE Advanced Scientific Computing Research User Facility. The authors would also like to thank Wanli Yang and Jon Spear for

beamline support at the Advanced Light Source. The data presented are available upon request to saykally@berkeley.edu.

[1]M. Faubel, S. Schlemmer, and J. P. Toennies, Z. Phys. D: Atoms, Mol. Clust. **10**, 269 (1988).
[2]M. Faubel, B. Steiner, and J. P. Toennies, J. Chem. Phys. **106**, 9013 (1997).
[3]K. R. Wilson, B. S. Rude, T. Catalano, R. D. Schaller, J. G. Tobin, D. T. Co, and R. J. Saykally, J. Phys. Chem. B **105**, 3346 (2001).
[4]R. Golnak, K. Atak, E. Suljoti, K. F. Hodeck, K. M. Lange, M. A. Soldatov, N. Engel, and E. F. Aziz, Phys. Chem. Chem. Phys. **15**, 8046 (2013).
[5]K. M. Lange and E. F. Aziz, Chem. Soc. Rev. **42**, 6840 (2013).
[6]L. Weinhardt, O. Fuchs, M. Blum, M. Bär, M. Weigand, J. D. Denlinger, Y. Zubavichus, M. Zharnikov, M. Grunze, C. Heske, and E. Umbach, J. Electron Spectrosc. Relat. Phenom. **177**, 206 (2010).
[7]K. M. Lange, R. Könnecke, S. Ghadimi, R. Golnak, M. A. Soldatov, K. F. Hodeck, A. Soldatov, and E. F. Aziz, Chem. Phys. **377**, 1 (2010).
[8]O. Shih, A. H. England, G. C. Dallinger, J. W. Smith, K. C. Duffey, R. C. Cohen, D. Prendergast, and R. J. Saykally, J. Chem. Phys. **139**, 035104 (2013).
[9]K. R. Wilson, B. S. Rude, J. Smith, C. Cappa, D. T. Co, R. D. Schaller, M. Larsson, T. Catalano, and R. J. Saykally, Rev. Sci. Instrum. **75**, 725 (2004).
[10]D. N. Kelly, C. P. Schwartz, J. S. Uejio, A. M. Duffin, A. H. England, and R. J. Saykally, J. Chem. Phys. **133**, 101103 (2010).
[11]C. D. Cappa, J. D. Smith, B. M. Messer, R. C. Cohen, and R. J. Saykally, J. Phys. Chem. B **110**, 5301 (2006).
[12]B. Winter and M. Faubel, Chem. Rev. **106**, 1176 (2006).
[13]M. A. Brown, F. Vila, M. Sterrer, S. Thürmer, B. Winter, M. Ammann, J. J. Rehr, and J. A. van Bokhoven, J. Phys. Chem. Lett. **3**, 1754 (2012).
[14]K. R. Wilson, M. Cavalleri, B. S. Rude, R. D. Schaller, A. Nilsson, L. G. M. Pettersson, N. Goldman, T. Catalano, J. D. Bozek, and R. J. Saykally, J. Phys. Condens. Matter **14**, L221 (2002).
[15]C. D. Cappa, J. D. Smith, K. R. Wilson, and R. J. Saykally, J. Phys. Condens. Matter **20**, 205105 (2008).
[16]C. D. Cappa, J. D. Smith, B. M. Messer, R. C. Cohen, and R. J. Saykally, J. Phys. Chem. B **110**, 1166 (2006).
[17]E. F. Aziz, N. Ottosson, S. Eisebitt, W. Eberhardt, B. Jagoda-Cwiklik, R. Vácha, P. Jungwirth, and B. Winter, J. Phys. Chem. B **112**, 12567 (2008).
[18]E. F. Aziz, M. Freiwald, S. Eisebitt, and W. Eberhardt, Phys. Rev. B **73**, 075120 (2006).
[19]K. M. Lange, A. Kothe, and E. F. Aziz, Phys. Chem. Chem. Phys. **14**, 5331 (2012).
[20]D. Chandler, J. D. Weeks, and H. C. Anderson, Science **220**, 787 (1983).
[21]G. Venturi, F. Formisano, G. J. Cuello, M. R. Johnson, E. Pellegrini, U. Bafile, and E. Guarini, J. Chem. Phys. **131**, 034508 (2009).
[22]M. Mondello and G. S. Grest, J. Chem. Phys. **103**, 7156 (1995).
[23]K. Griesbaum, A. Behr, D. Biedenkapp, H.-W. Voges, D. Garbe, C. Paetz, G. Collin, D. Mayer, H. Höke, and R. Schmidt, *Ullmann's Encyclopedia of Industrial Chemistry* (Wiley-VCH Verlag GmbH and Co., KGaA, 2000).
[24]O. Fuchs, F. Maier, L. Weinhardt, M. Weigand, M. Blum, M. Zharnikov, J. Denlinger, M. Grunze, C. Heske, and E. Umbach, Nucl. Instrum. Methods Phys. Res. A **585**, 172 (2008).
[25]M. Nagasaka, T. Hatsui, T. Horigome, Y. Hamamura, and N. Kosugi, J. Electron Spectrosc. Relat. Phenom. **177**, 130 (2010).
[26]P. Jiang, J.-L. Chen, F. Borondics, P.-A. Glans, M. W. West, C.-L. Chang, M. Salmeron, and J. Guo, Electrochem. Commun. **12**, 820 (2010).
[27]W. Bambynek, B. Crasemann, R. W. Fink, H. U. Freund, H. Mark, C. D. Swift, R. E. Price, and P. V. Rao, Rev. Mod. Phys. **44**, 716 (1972).
[28]M. O. Krause, J. Phys. Chem. Ref. Data **8**, 307 (1979).
[29]J. Pfaff, M. H. Begemann, and R. J. Saykally, Mol. Phys. **52**, 541 (1984).
[30]M. H. Begemann and R. J. Saykally, Opt. Commun. **40**, 277 (1982).
[31]A. Duffin and R. Saykally, J. Phys. Chem. C **111**, 12031 (2007).
[32]A. Duffin and R. Saykally, J. Phys. Chem. C **112**, 17018 (2008).
[33]D. N. Kelly, R. K. Lam, A. M. Duffin, and R. J. Saykally, J. Phys. Chem. C **117**, 12702 (2013).
[34]H. Bekker, H. J. C. Berendsen, E. J. Dijkstra, S. Achterop, R. van Drunen, D. van der Spoel, A. Sijbers, H. Keegstra, B. Reitsma, and M. K. R. Renardus, *Physics Computing* (World Scientific Publishing Company, Singapore, 1993), Vol. 92, pp. 252–256.
[35]H. J. C. Berendsen, D. van der Spoel, and R. van Drunen, Comput. Phys. Commun. **91**, 43 (1995).
[36]E. Lindahl, B. Hess, and D. van der Spoel, Mol. Model. Annu. **7**, 306 (2001).
[37]D. Van Der Spoel, E. Lindahl, B. Hess, G. Groenhof, A. E. Mark, and H. J. C. Berendsen, J. Comput. Chem. **26**, 1701 (2005).
[38]B. Hess, C. Kutzner, D. van der Spoel, and E. Lindahl, J. Chem. Theory Comput. **4**, 435 (2008).
[39]W. L. Jorgensen, D. S. Maxwell, and J. Tirado-Rives, J. Am. Chem. Soc. **118**, 11225 (1996).
[40]G. A. Kaminski, R. A. Friesner, J. Tirado-Rives, and W. L. Jorgensen, J. Phys. Chem. B **105**, 6474 (2001).
[41]M. L. P. Price, D. Ostrovsky, and W. L. Jorgensen, J. Comput. Chem. **22**, 1340 (2001).
[42]S. W. I. Siu, K. Pluhackova, and R. A. Bockmann, J. Chem. Theory Comput. **8**, 1459 (2012).
[43]D. Prendergast and G. Galli, Phys. Rev. Lett. **96**, 215502 (2006).
[44]P. Giannozzi, S. Baroni, N. Bonini, M. Calandra, R. Car, C. Cavazzoni, D. Ceresoli, G. L. Chiarotti, M. Cococcioni, I. Dabo, A. Dal Corso, S. de Gironcoli, S. Fabris, G. Fratesi, R. Gebauer, U. Gerstmann, C. Gougoussis, A. Kokalj, M. Lazzeri, L. Martin-Samos, N. Marzari, F. Mauri, R. Mazzarello, S. Paolini, A. Pasquarello, L. Paulatto, C. Sbraccia, S. Scandolo, G. Sclauzero, A. P. Seitsonen, A. Smogunov, P. Umari, and R. M. Wentzcovitch, J. Phys. Condens. Matter **21**, 395502 (2009).
[45]J. P. Perdew, K. Burke, and M. Ernzerhof, Phys. Rev. Lett. **77**, 3865 (1996).
[46]K. Momma and F. Izumi, J. Appl. Crystallogr. **41**, 653 (2008).
[47]Lord Rayleigh, Proc. London Math. Soc **10**, 4–13 (1878).
[48]Lord Rayleigh, Philos. Mag. Ser. 5 **34**, 145 (1892).
[49]C. D. Cappa, J. D. Smith, K. R. Wilson, B. M. Messer, M. K. Gilles, R. C. Cohen, and R. J. Saykally, J. Phys. Chem. B **109**, 7046 (2005).
[50]K. R. Wilson, M. Cavalleri, B. S. Rude, R. D. Schaller, T. Catalano, A. Nilsson, R. J. Saykally, and L. G. M. Pettersson, J. Phys. Chem. B **109**, 10194 (2005).
[51]J.-H. Guo, Y. Luo, A. Augustsson, S. Kashtanov, J.-E. Rubensson, D. K. Shuh, H. Ågren, and J. Nordgren, Phys. Rev. Lett. **91**, 157401 (2003).
[52]S. Kashtanov, A. Augustson, J.-E. Rubensson, J. Nordgren, H. Agren, J.-H. Guo, and Y. Luo, Phys. Rev. B **71**, 104205 (2005).
[53]H. Sun, J. Phys. Chem. B **102**, 7338 (1998).
[54]W. L. Jorgensen, J. D. Madura, and C. J. Swenson, J. Am. Chem. Soc. **106**, 6638 (1984).
[55]J. W. Mutoru, W. Smith, C. S. O'Hern, and A. Firoozabadi, J. Chem. Phys. **138**, 024317 (2013).